Mesenchymal Chondrosarcoma of the Head and Neck with HEY1::NCOA2 Fusion

Xu, Bin; Rooper, Lisa M; Dermawan, Josephine K; Zhang, Yanming; Suurmeijer, Albert J H; Dickson, Brendan C; Demicco, Elizabeth G; Antonescu, Cristina R

Published in:
GENES CHROMOSOMES & CANCER

DOI:
10.1002/gcc.23075

Publication date:
2022

Received: 28 March 2022 | Revised: 24 May 2022 | Accepted: 26 May 2022

DOI: 10.1002/gcc.23075

RESEARCH ARTICLE

WILEY

Mesenchymal chondrosarcoma of the head and neck with *HEY1::NCOA2* fusion: A clinicopathologic and molecular study of 13 cases with emphasis on diagnostic pitfalls

Bin Xu[1] | Lisa M. Rooper[2] | Josephine K. Dermawan[1] | Yanming Zhang[1] | Albert J. H. Suurmeijer[3] | Brendan C. Dickson[4] | Elizabeth G. Demicco[4] | Cristina R. Antonescu[1]

[1]Department of Pathology and Laboratory Medicine, Memorial Sloan Kettering Cancer Center, New York City, New York, USA

[2]Department of Pathology, Johns Hopkins University School of Medicine, Baltimore, Maryland, USA

[3]Department of Pathology and Laboratory Medicine, University Medical Center Groningen, University of Groningen, Groningen, The Netherlands

[4]Department of Pathology & Laboratory Medicine, Mount Sinai Hospital & Laboratory Medicine and Pathobiology, University of Toronto, Toronto, Ontario, Canada

Correspondence
Cristina R. Antonescu, Department of Pathology and Laboratory Medicine, Memorial Sloan Kettering Cancer Center, 1275 York Avenue, New York, NY 10065, USA.
Email: antonesc@mskcc.org

Funding information
National Institutes of Health

Abstract

Background: Mesenchymal chondrosarcoma (MCS) is a rare translocation-associated sarcoma, driven by a canonical *HEY1::NCOA2* fusion. The tumors typically have a biphasic phenotype of primitive small blue round cells intermixed with hyaline cartilage. The head and neck (HN) region is a common site for MCS, accounting for 12–45% of all cases reported.

Aims: We assembled a relatively large cohort of 13 molecularly confirmed HN MCS for a detailed clinicopathologic analysis. The underlying fusion events were determined using fluorescence in situ hybridization and/or targeted RNA sequencing.

Results: The median age of presentation was 19 years. Five MCSs (39%) had an intraosseous presentation (skull, maxilla, palate, and mandible), while the remaining eight cases occurred in the brain/meninges, orbit, and nasal cavity. Microscopically, HN MCSs were characterized by primitive round cells arranged in a distinctive nested architecture and a rich staghorn vasculature. A cartilaginous component of hyaline cartilage islands and/or single chondrocytes were present in 69% cases. A combined immunoprofile of CD99(+)/SATB2(+)/CD34(−)/STAT6(−) was typically noted. As this immunoprofile is non-specific, the referral diagnoses in cases lacking a cartilaginous component included Ewing sarcoma family and osteosarcoma. Among the seven patients with follow-up data, three developed distant metastasis and one died of disease.

Conclusion: HN MCS may arise at intra- or extra-osseous sites. The HN MCS appears to have a more prolonged survival compared other MCS sites. Testing for *HEY1::NCOA2* fusion is recommended in HN tumors with nested round cell morphology and staghorn vasculature that lack a distinctive cartilaginous component.

KEYWORDS
chondrosarcoma, head and neck, *HEY1::NCOA2* fusion, mesenchymal chondrosarcoma

1 | INTRODUCTION

Mesenchymal chondrosarcoma (MCS) is a rare high-grade sarcoma displaying a biphasic phenotype of primitive small blue round to spindle cells intermixed with islands or single cells of hyaline cartilage.[1] Despite its WHO classification under chondrosarcoma group, a cartilaginous component might be scant, ill-defined, or even absent in a subset of cases, particularly in small samples.[2] In contrast

TABLE 1 Clinicopathologic features and outcome of head and neck mesenchymal chondrosarcoma

N	Age/ sex	Anatomic site	Intraosseous component	*NCOA2* fusion	Specimen type	Tumor size (cm)	MI	Staghorn vessels	Nested architecture	Cartilage/ chondrocytes	Necrosis	Treatment	Metastasis	Outcome
1	19/M	Brain (cerebellum)	Extraosseous	*HEY1::NCOA2*	Biopsy	NA	2	Present	Present	Cartilage	Absent	Sx, CRT	Cervical spine	AWD (48 m)
2	49/F	Brain (parietal lobe)	Extraosseous	*HEY1::NCOA2*	Resection	NA	10	Present	Absent	Absent	Present	NA	NA	NA
3	23/F	Intradural (frontal/ temporal)	Extraosseous	*HEY1::NCOA2*	Resection	NA	4	Present	Present	Cartilage	Present	NA	NA	NA
4	21/F	Intradural (cervical spine)	Extraosseous	*NCOA2* fusion	Resection	NA	NA	Present	Present	Absent	Absent	NA	NA	NA
5	28/F	Brain/skull	Intraosseous	*HEY1::NCOA2*	Biopsy	NA	6	Focal	Present	Absent	Absent	NA	None	NED (60 m)
6	16/F	Brain/skull (posterior fossa)	Intraosseous	*HEY1::NCOA2*	Resection	NA	21	Present	Present	Cartilage	Absent	Sx, CRT	Lung, retroperitoneum	AWD (193 m)
7	6/M	Orbit	Extraosseous	*NCOA2* fusion	Resection	3	25	Present	Present	Cartilage	Absent	Sx, CT	None	NED (150 m)
8	8/M	Orbit	Extraosseous	*NCOA2* fusion	Biopsy	NA	1	Focal	Focal	Cartilage	Absent	NA	NA	NA
9	14/F	Nasal cavity	Extraosseous	*NCOA2* fusion	Resection	6.6	0	Focal	Absent	Cartilage	Present	Sx, CRT	None	NED (60 m)
10	9/M	Nasal cavity	Extraosseous	*HEY1::NCOA2*	Biopsy	3	10	Present	Absent	Absent	Absent	NA	NA	NA
11	54/F	Maxilla	Intraosseous	*NCOA2* fusion	Biopsy	4, 3	1	Present	Present	Cartilage	Absent	NA	Cervical lymph nodes, spine, bone	DOD (24 m)
12	18/F	Mandible	Intraosseous	*NCOA2* fusion	Resection	4.4	2	Focal	Focal	Cartilage	Absent	Sx, CT	None	NED (12 m)
13	20/F	Oral cavity (palate/maxilla)	intraosseous	*HEY1::NCOA2*	Excision	2.6	4	Present	Present	Cartilage	Absent	NA	NA	NA

Abbreviations: AWD, alive with disease; CRT, chemoradiation therapy; CT, chemotherapy; DOD, dead of disease; F, female; M, male; MI, Mitotic index (per 10 high power fields); N, Patients' number; NA, not available; NED, no evidence of disease; Sx, Surgery.

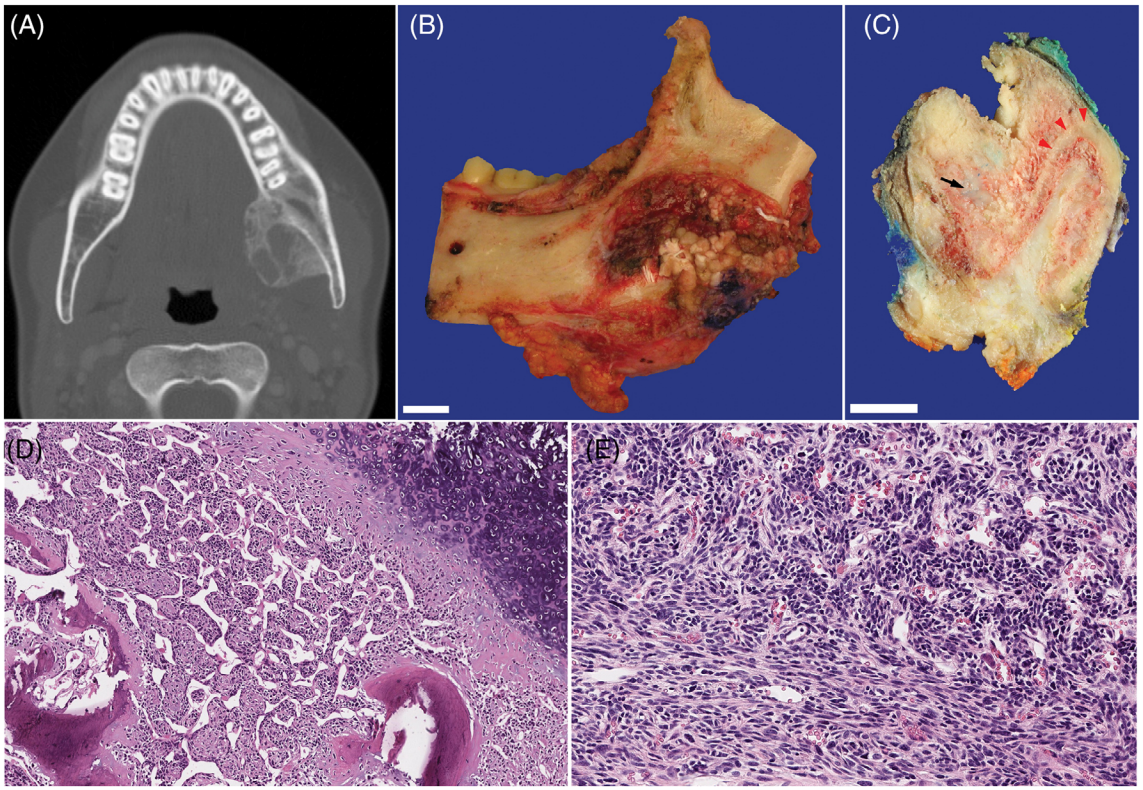

FIGURE 1 A mesenchymal chondrosarcoma of the mandible in an 18-year-old female patient (case #12). (A) A computer tomography (CT) scan shows a large heterogenous intraosseous mass centered at the junction of the body and ascending ramus eroding through the cortex with a large calcified extraosseous component. (B and C) Macroscopic examination. External view (B) and cross section (C) of the tumor showed breach of the mandibular cortex (red arrowheads) and involvement of adjacent soft tissue. Cartilaginous matrix (black arrow) was grossly visible. Scale bar: 1 cm. (D) Microscopically, the tumor permeated between the native bone trabeculae. Abrupt transition between the hyaline cartilage (top right) and a primitive small blue cell component (bottom left) was seen. The small blue cells are arranged in a nested architecture separated by prominent staghorn vasculature. (E) At high power, the tumor cells contained ovoid to round nuclei with scant cytoplasm arranged in nests or trabeculae. Areas of spindle cells forming loose fascicles (bottom) are also present in this tumor.

with most conventional chondrosarcomas that occur in the bone, MCS show a wide anatomic distribution, with either skeletal, soft tissue, intracranial, or visceral presentations. The head and neck (HN) region is a common location of MCS, accounting for 12–45% of the cases.[3–7] HN MCS may originate from the craniofacial bone (such as mandible, maxilla, and skull), cervical spine, extraosseous soft tissue (such as sinonasal tract, neck soft tissue, and orbit), or intracranially.[3–9]

In 2012, the molecular alterations of MCS were characterized, with most cases (at least 80%) harboring a *HEY1*::*NCOA2* canonical fusion.[10–12] An additional case report of a cerebral MCS showing an *IRF2BP2*::*CDX1* variant fusion[13] was documented. However, this result has not been yet validated as a recurrent genetic event by other investigators.

In this study, we describe the clinicopathologic features and outcome in an a large retrospective series of 13 HN-MCS with confirmed *HEY1*::*NCOA2* fusion. We also stress the challenging differential diagnosis of this entity at HN location, in particular when faced with limited tissue biopsies, lack of cartilaginous component, and non-specific immunoprofile.

2 | MATERIALS AND METHODS

2.1 | Patients' selection and clinicopathologic review

The study was approved by the Institutional Review Board (IRB) of each participating site. Candidate cases were retrieved from the pathology archives of Memorial Sloan Kettering Cancer Center (New York, NY, USA, $n = 8$), Johns Hopkins University (Baltimore, MD, USA, $n = 3$), University Medical Center Groningen (Groningen, Netherlands, $n = 1$), and Mount Sinai Hospital (Toronto, ON, Canada, $n = 1$). All cases were centrally reviewed by two pathologists (BX and CRA) to gather relevant pathologic parameters. A chart review was conducted at each individual site to collect demographic and outcome data. The 5-year and 10-year overall survival and disease-specific survival were calculated using SPSS software 24.0 (IBM Corporation, Armonk, NY, U.S.).

Immunohistochemistry studies were performed in a subset of cases using the following primary antibodies: CD99 (clone: O13, dilution 1:800, Labcorp, Princeton, NJ, USA), CD34 (clone: QBEnd-10,

ready to use RTU, Ventana, Roche diagnostics, Oro Valley, AZ, UA), SATB2 (clone: EP281, dilution 1:00, Cell Marque corporation, Rocklin, CA, USA), and STAT6 (catalog number: SC-621, dilution 1:2500, Santa Cruz Biotechnology, Dallas, TX, USA).

2.2 | Targeted RNA sequencing and FISH detection of NCOA2 gene alterations

NCOA2-related gene fusions/rearrangements were detected in all cases using RNA sequencing ($n = 7$) and/or fluorescence in situ hybridization (FISH, $n = 9$) as previously described.[14,15] Cases without material for molecular testing were excluded from the current study.

In brief, RNA sequencing was performed using either the Illumina TruSight RNA fusion panel targeting 507 known fusion-related gene targets (Illumina, San Diego, CA, US) and Illumina MiSeq V.3 platform,[14] or ARCHER RNA sequencing platform, a clinical molecular diagnostic essay performed in a CLIA-accredited laboratory utilizing multiplex polymerase chain reaction (PCR) to detect oncogenic fusion transcripts involving 123 genes.[15]

FISH for *NCOA2* gene rearrangements was performed using either a *NCOA2* break apart probe set (Empire Genomics, Williamsville, NY, USA) or custom bacterial artificial chromosome clone probes designed to flank the target genes based on the UCSC genome browser (http://genome.ucsc.edu/).[10]

3 | RESULTS

3.1 | Clinicopathologic and radiographic features

The clinicopathologic characteristics and outcome of the study cohort are listed in Table 1. The median age at diagnosis was 19 years (range: 6–54 years). The female to male ratio was 9:4 (2.25:1). Five tumors (39%) had an intraosseous component and were favored to be originated from bone, including two tumors involving skull, two affecting maxillary bone, one arising from the mandible (Figure 1). The remaining eight tumors (61%) were extra-osseous, involving brain/meninges ($n = 4$, Figure 2), orbital soft tissue ($n = 2$), and nasal cavity ($n = 2$). Six tumors (46%) affected the central nervous system as intracranial ($n = 5$) or intraspinal ($n = 1$) lesions.

Computed tomography images were available in five cases (cases #6, #7, #9, #12, and #13), four (80%) of which contained calcified matrix. Most tumors were described as destructive, lobulated with a mixed soft tissue density, and chondroid calcifications. The tumors often involved of the nasal cavity or maxillary sinuses, with erosion of nearby bony structures, for example, orbital floor or sphenoid wing. The clivus was typically spared. The main differential diagnosis radiographically was that of a chondrosarcoma. Macroscopically, these tumors often contained matrix material, either as course calcification or as cartilaginous matrix.

Histologically, MCS had a biphasic appearance in 69% of cases, composed of a primitive small round to spindle cell component arranged in nests or tightly packed short fascicles, intermixed with often small islands of hyaline cartilage. Occasionally, single chondrocytes might also be seen (Figure 3C). Some cases in addition showed foci of ill-defined cartilaginous tissue in the form of chondromyxoid matrix. Among the nine cases with cartilaginous component, the transition between small blue cell component and cartilaginous component was either abrupt/well-demarcated ($n = 7$), or gradual ($n = 7$).

A cartilaginous component was completely absent in four cases (one biopsy and three resections, 31%), presenting a significant challenge to distinguish from other primitive small blue round cell tumors.

Another characteristic histologic feature was the presence of branching staghorn (a.k.a. hemangiopericytoma-like) vasculature. Such vascular pattern was seen in all cases, including six patients with only small biopsy material available, although the presence of such features could be focal in some cases (four out of 13 in our series, 31%).

Nested architecture was presented in all but three cases. Tumor necrosis was relatively uncommon, detected in three (23%)

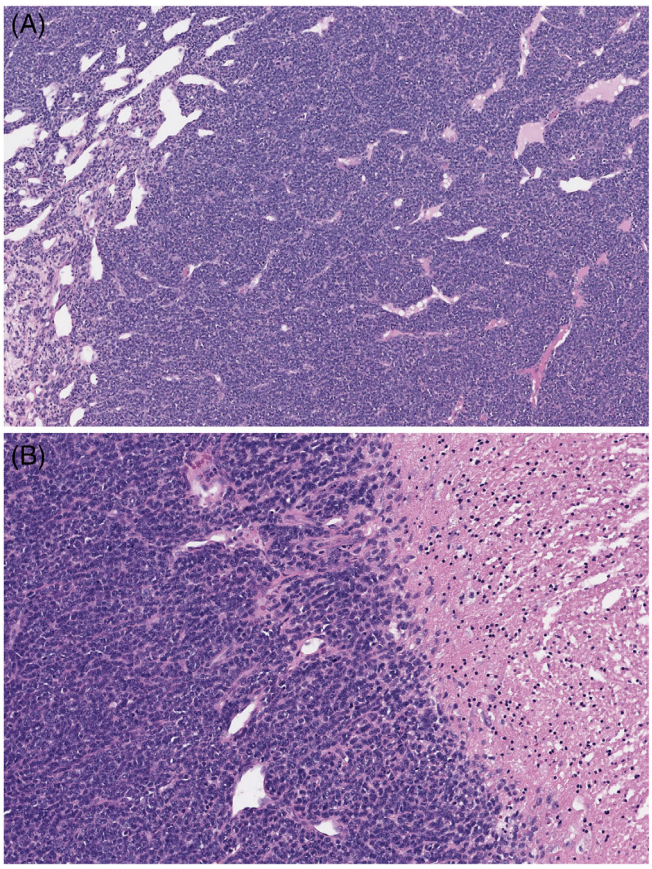

FIGURE 2 An intracranial extra-osseous mesenchymal chondrosarcoma involving the parietal lobe of a 49-year-old female patient (case #2). (A) The tumor is composed entirely of undifferentiated small blue round cells arranged in nests and trabeculae. Branching staghorn vessels were noted throughout. No cartilaginous matrix or chondrocytes were identified in the resection specimen. (B) The tumor shows multifocal comedo-type tumor necrosis (right).

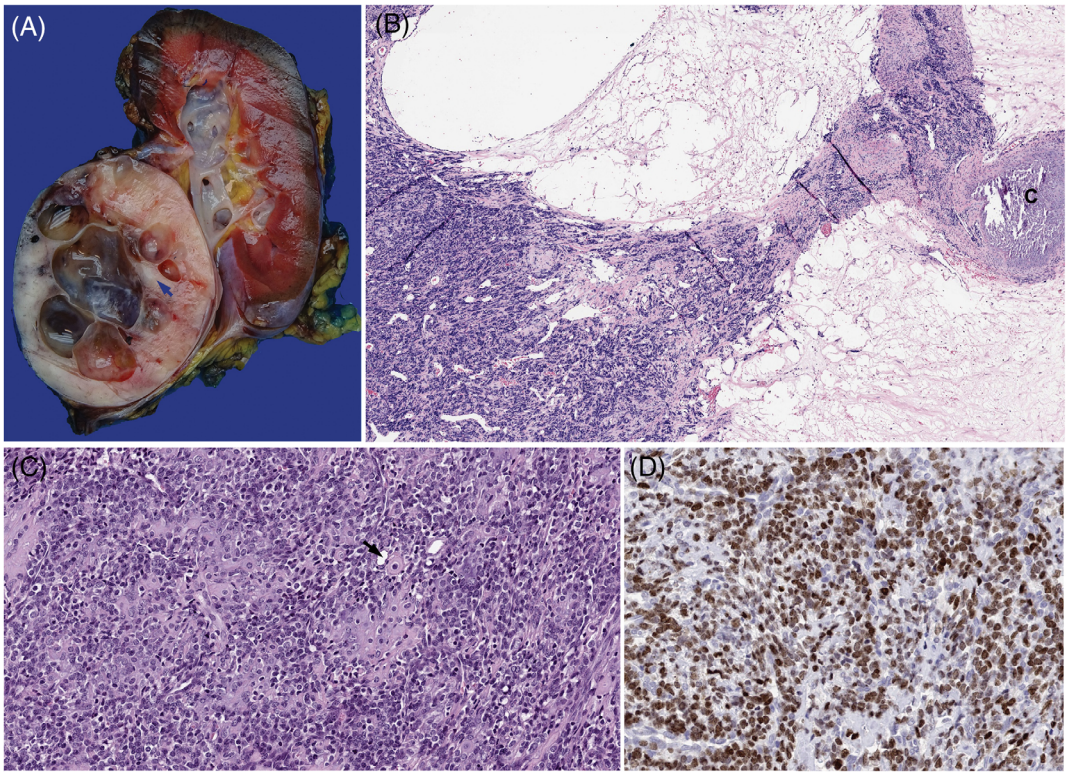

FIGURE 3 A late metastatic recurrence occurred 13 years after the initial diagnosis of a mesenchymal chondrosarcoma involving brain and skull base (Case #6). (A) Macroscopically, the retroperitoneal metastasis presented as a 7.8 cm well-circumscribed mass compressing but not invading the renal pelvis and ureter. Areas of cartilaginous matrix (blue arrow) and cystic change are seen. (B) At low power, the tumor is composed of small blue round cells arranges as nest and trabeculae in a fibrotic stroma. Staghorn vasculature, calcified hyaline cartilage [C], and cystic changes were seen. (C) at high power, foci of ill-defined chondroid matrix, and scattered single chondrocytes (arrow) were noted admixed with primitive small blue round cells. (D) The tumor is diffusely positive for SATB2.

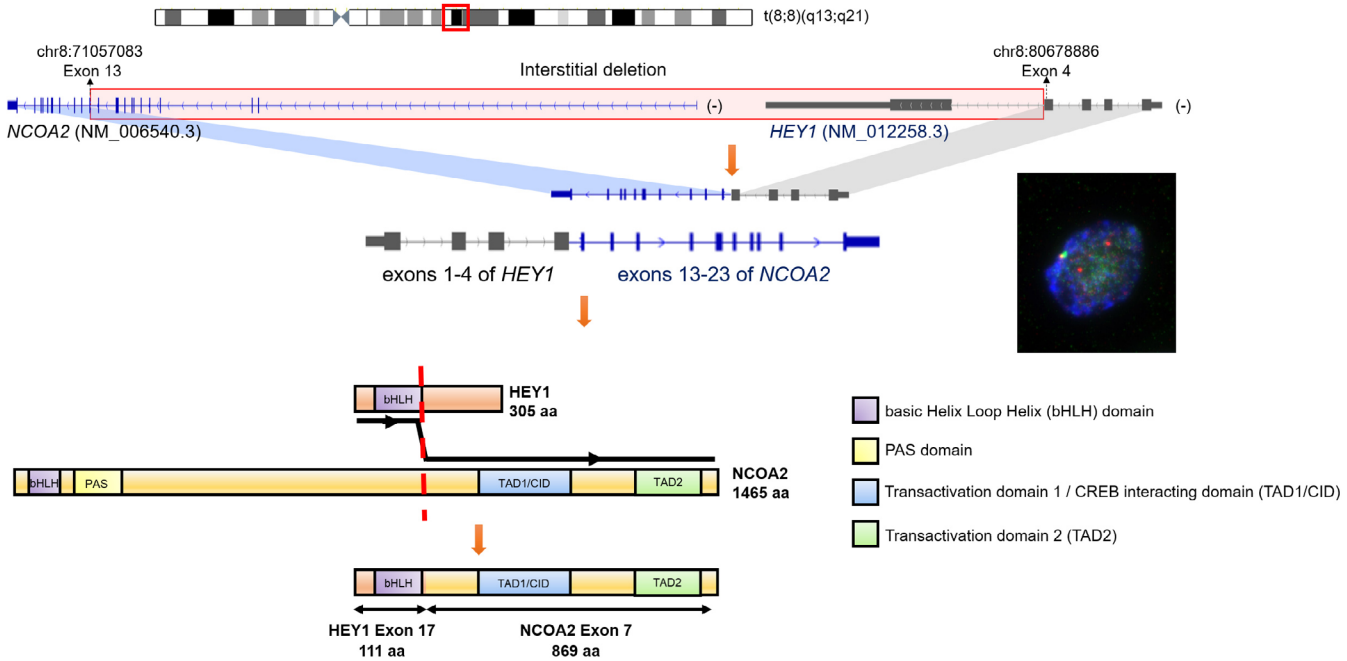

FIGURE 4 *HEY1*::*NCOA2* fusion in mesenchymal chondrosarcoma. An interstitial deletion resulting in an in-frame fusion between genes *HEY1* exon 4 and *NCOA2* exon 13 was detected by ARCHER RNA sequencing platform. Insert: Fluorescence in situ hybridization analysis of *NCOA2* shows an extra signal for the 3′ probe (red), and loss of the 5′ probe (green), indicative of an interstitial deletion between *HEY1* and *NCOA2*.

cases. The mitotic activity varied widely in MCS, ranging from nil to 25 per high power fields (median: 4).

Immunohistochemistry was performed in selected cases. MCS was frequently positive for SATB2 (3 out of 3 cases, 100%) and CD99 (3/3, 100%). STAT6 (0/2) and CD34 (0/6) were negative in tested cases.

3.2 | Treatment and clinical outcomes

Treatment and outcome information were only available in a subset of cases ($n = 5$ and $n = 7$ respectively). All patients received surgical resection and chemotherapy. Two patients additionally received adjuvant radiation therapy. The commonly used chemotherapy was an Ewing sarcoma regimen (vincristine, doxorubicin, and cyclophosphamide alternating with etoposide and ifosfamide, $n = 4$). One of these patients received this regimen in neoadjuvant setting without appreciable treatment effects in the resection specimen. The fifth patient received neoadjuvant high-dose cyclophosphamide, doxorubicin, and vincristine with no response, and was treated with etoposide and ifosfamide post-operatively.

Outcome data were available in seven patients with a median follow up of 60 months (range: 12–193 months). Three patients developed distant metastasis, including one patient who developed late distant recurrence 13 years after the initial resection (Figure 3). At the time of last follow up, there was one disease-related death in a 54-year-old female patient with a maxillary intraosseous tumor and widely metastatic disease to cervical lymph nodes, spine, and multiple bones. The 5-year and 10-year overall survival and disease-specific survival were 83%.

3.3 | HEY1::NCOA2 Fusion

The presence of diagnostic *HEY1*::*NCOA2* fusion was detected in all cases using FISH and/or RNA sequencing. RNA sequencing showed an interstitial deletion resulting in an in-frame fusion between *HEY1* exon 4 and *NCOA2* exon 13. The resulting fusion product retained the basic Helix Loop Helix (bHLH) domain of HEY1 and the transactivation domains of NCOA2 (TAD1/CID, transactivation domain 1/CREB interacting domain and TAD2, transactivation domain 2) (Figure 4).

4 | DISCUSSION

The HN region is a common presentation for MCS, accounting for approximately 12–45% of all MCS cases reported.[3–7] Dedicated series on HN MCS are sparse in the literature. We identified only two studies: one by Vencio et al. reporting 15 cases of MCSs arising in the jaw bones,[9] the other by Knott et al. including 13 cases of MCS from the sinonasal tract,[8] neither of which included confirmed diagnosis by molecular assays. We herein described a large series of 13 cases of HN MCS with molecular confirmation of the underlying *HEY1*::*NCOA2* fusion.

Within the HN area, the most affected sites of MCS are the craniofacial bones, such as mandible, maxilla, and skull/skull base.[6,9] However, MCS has also been reported at extraosseous sites in 10% to 73% of cases.[5–7] The HN soft tissue site that may be involved by MCS includes meninges/brain, orbit, neck soft tissue, pterygopalatine fossa, nasal cavity, thyroid, and paranasal sinus.[8,16–18] In addition to these extraosseous sites, we herein reported a case of MCS originating from the palate. In our series, the rate of extraosseous MCS was high (61%), highlighting the need to include MCS in the differential diagnosis of a HN primitive small blue round cell tumor, regardless of the bone involvement and the anatomical location.

The median age of presentation was 19 years, slightly younger than that median age of 29–32 years reported in previous studies.[5,8,19] However, most studies, including the present one, have shown that patients with MCS have a peak incidence around second and third decade, but a wide age range is reported, from 1 to 83 years.[3–6,8,9,17,19]

Overall, MCS is associated with an aggressive clinical course. Several recent studies, including a meta-analysis of 107 patients,[20] a Surveillance, Epidemiology, and End Results (SEER)-based study of 205 patients,[21] and a European Musculoskeletal Oncology Society study of 113 patients from 17 centers,[5] showed a 5-year overall survival of 51–71%, and a 10-year overall survival of 43–54%. HN MCSs appear to follow a more indolent course, possibly due to an earlier detection of symptoms compared to non-HN cases[22]; with a 5-year and 10-year overall survival of jawbone MCS, for example, being 82% and 56%, respectively. Similarly, the 5-year and 10-year overall survival of the current series was 83% and 83%, respectively, although the follow up data was relatively limited. However, not all studies comparing the survival of MCS by anatomic sites support such an observation. While the study by the European Musculoskeletal Oncology Society reported similar outcome of MCSs from HN and trunk,[5] two studies (one based on SEER data, and the other by the Japanese Musculoskeletal Oncology Group) showed that MCS from the trunk was associated with decreased survival compared to other locations (including HN).[4,21] The 5-year OS was 74% for cranial MCS, compared with 37% for axial MCS.[21]

Two patients in our series received neoadjuvant chemotherapy, both of whom showed no appreciable treatment response. Similarly, Huvos et al. showed no response to pre-operative high dose methotrexate-based chemotherapy in four MCS patients.[3] Tsuda et al. reported stable disease in three cases and partial response in one case of MCS treated with neoadjuvant chemotherapy.[4] Overall, the benefit of neoadjuvant chemotherapy for MCS remains unproven.

Delayed recurrence and metastasis are well-documented in MCS.[22] Knott et al., for example, described a patient with sinonasal MCS who developed distant metastasis 24 years after the initial diagnosis.[8] Similarly, in our series, a 16-year-old girl developed delayed metastasis to lung and retroperitoneum 13 years after the initial resection of a brain/skull MCS (case #6, Figure 3). Given the likelihood of delayed recurrence, long-term follow up is required for patients diagnosed with HN MCS.

MCS is prone to misdiagnosis, especially when the classic histologic appearance of a biphasic tumor with mature hyaline cartilage is absent. For example, Knott et al. reported that 62% of the MCSs were misdiagnosed, most commonly as solitary fibrous tumor. Indeed, solitary fibrous tumor constitutes a major differential diagnosis of MCS, as both tumors typically contain branching staghorn (a.k.a. hemangiopericytoma-like) vasculature and small round to spindle cell cytomorphology. In the present study, the staghorn vascular pattern was observed either focally or diffusely in all MCSs, including in small biopsy samples. Fortunately, our data showed that MCS were universally negative for CD34 and STAT6, two immunohistochemical stains that are typically positive in solitary fibrous tumors.[1,23,24] Similarly, Demicco et al. showed that STAT6 was negative in six MCSs tested.[24] Therefore, a combined immunohistochemistry studies using CD34 and STAT6 may be used as the initial work-up to distinguish MCS and solitary fibrous tumors.

Another differential diagnosis for MCS is Ewing sarcoma, a primitive small blue round cell tumor. Previous studies and the current series have shown that CD99 membranous immunopositivity can be seen in (near) all MCS,[25,26] making it an unreliable ancillary marker to differentiate between MCS and Ewing sarcoma. On the other hand, SATB2 immunostain may be somewhat useful as part of the immunohistochemical work up in distinguishing these two tumors. SATB2 immunopositivity can be seen in 47% to 52% of chondrosarcoma, including MCS.[27,28] Our series shows that diffuse SATB2 immunopositivity is common in MCS. In contrast, SATB2 is uncommon in Ewing sarcoma, being positive in merely 1.7% of cases.[27]

Osteosarcoma, especially the small cell and chondroblastic subtype, may also be included in the differential diagnosis of MCS, as both sarcomas may originate intraosseously, show mineralization/calcification on radiology and histology, express SATB2 diffusely, and contain small round/spindle cell or cartilaginous components.[1] A focal hemangiopericytoma-like vasculature may also present focally in small cell osteosarcoma. The absence of lace-like osteoid production and the presence of *HEY1::NCOA2* fusion are essential to establish the diagnosis of MCS.

When the initial histologic assessment and immunohistochemistry studies yield inconclusive results, diagnostic molecular tests to evaluate underlying fusion events is essential to establish a definite diagnosis. *HEY1::NCOA2* fusion is the characteristic molecular event for MCS.[10,11] This canonical fusion has been exclusively associated with MCS, except for an intriguing single case report with hybrid sclerosing epithelioid fibrosarcoma/low grade fibromyxoid sarcoma morphology from the intestine harboring a *HEY1::NCOA2* fusion.[29] All HN MCS included in our series showed the presence of an *HEY1::NCOA2* fusion. In our series, four cases (31%) contained exclusively primitive small blue round cells without cartilaginous component. The diagnosis of MCS was rendered based on the detection of the underlying fusion. No *IRF2BP2::CDX1* fusion was detected in our series by RNA sequencing, thus raising questions if this alternative fusion previously reported in a single case of cerebral MCS[13] represents a recurrent genetic event.

In conclusion, HN MCS may show various clinical presentations, involving the craniofacial bones, meninges, brain, orbit, sinonasal tract, and oral cavity. MCS represents a primitive small blue round cell tumor commonly showing evidence of cartilaginous component, staghorn vessels, nested architecture, and variable mitotic activity. It often demonstrates a CD99 (+)/SATB2(+)/STAT6 (−)/CD34(−) non-specific immunoprofile. All HN MCSs in our series harbored the pathognomonic *HEY1::NCOA2* fusion, which served as a useful diagnostic molecular signature especially when the typical biphasic histology with hyaline cartilage was absent.

AUTHOR CONTRIBUTIONS

Conception of the study: BX, CRA. Pathology and chart review: BX, LMR, AJHS, EGD, CRA. FISH analysis: YZ, CRA. RNA sequencing: JKD, BCD. Manuscript drafting: BX. Manuscript editing: BX, LMR, JKD, YZ, AJHS, BCD, EGD, CRA.

ACKNOWLEDGMENTS

Research reported in this publication was supported in part by the Cancer Center Support Grant of the National Institutes of Health/National Cancer Institute under award number P30 CA008748 (BX, CRA) and P50 CA217694 (CRA). The content is solely the responsibility of the authors and does not necessarily represent the official views of the National Institutes of Health.

CONFLICT OF INTEREST

The authors have disclosed that they have no significant relationships with, or financial interest in any commercial companies pertaining to this article.

DATA AVAILABILITY STATEMENT

The data that support the findings of this study are available on request from the corresponding author. The data are not publicly available due to privacy or ethical restrictions.

ORCID

Bin Xu https://orcid.org/0000-0003-4638-9835
Josephine K. Dermawan https://orcid.org/0000-0002-1139-2914
Brendan C. Dickson https://orcid.org/0000-0003-2269-6216
Cristina R. Antonescu https://orcid.org/0000-0002-9717-8205

REFERENCES

1. WHO Classification of Tumours Editorial Board. *WHO classification of tumours of soft tissue and bone*. 5th edition ed. International Agency for Research on Cancer; 2020.
2. Folpe AL, Graham RP, Martinez A, Schembri-Wismayer D, Boland J, Fritchie KJ. Mesenchymal chondrosarcomas showing immunohistochemical evidence of rhabdomyoblastic differentiation: a potential diagnostic pitfall. *Hum Pathol*. 2018;77:28-34.
3. Huvos AG, Rosen G, Dabska M, Marcove RC, Mesenchymal chondrosarcoma. A clinicopathologic analysis of 35 patients with emphasis on treatment. *Cancer*. 1983;51(7):1230-1237.
4. Tsuda Y, Ogura K, Hakozaki M, et al. Mesenchymal chondrosarcoma: a Japanese Musculoskeletal Oncology Group (JMOG) study on 57 patients. *J Surg Oncol*. 2017;115(6):760-767.
5. Frezza AM, Cesari M, Baumhoer D, et al. Mesenchymal chondrosarcoma: prognostic factors and outcome in 113 patients. A European Musculoskeletal Oncology Society study. *Eur J Cancer*. 2015;51(3):374-381.

6. Shakked RJ, Geller DS, Gorlick R, Dorfman HD. Mesenchymal chondrosarcoma: clinicopathologic study of 20 cases. *Arch Pathol Lab Med*. 2012;136(1):61-75.
7. Dantonello TM, Int-Veen C, Leuschner I, et al. Mesenchymal chondrosarcoma of soft tissues and bone in children, adolescents, and young adults: experiences of the CWS and COSS study groups. *Cancer*. 2008;112(11):2424-2431.
8. Knott PD, Gannon FH, Thompson LD. Mesenchymal chondrosarcoma of the sinonasal tract: a clinicopathological study of 13 cases with a review of the literature. *Laryngoscope*. 2003;113(5):783-790.
9. Vencio EF, Reeve CM, Unni KK, Nascimento AG. Mesenchymal chondrosarcoma of the jaw bones: clinicopathologic study of 19 cases. *Cancer*. 1998;82(12):2350-2355.
10. Wang L, Motoi T, Khanin R, et al. Identification of a novel, recurrent HEY1-NCOA2 fusion in mesenchymal chondrosarcoma based on a genome-wide screen of exon-level expression data. *Genes Chromosomes Cancer*. 2012;51(2):127-139.
11. Nakayama R, Miura Y, Ogino J, et al. Detection of HEY1-NCOA2 fusion by fluorescence in-situ hybridization in formalin-fixed paraffin-embedded tissues as a possible diagnostic tool for mesenchymal chondrosarcoma. *Pathol Int*. 2012;62(12):823-826.
12. El Beaino M, Roszik J, Livingston JA, et al. Mesenchymal chondrosarcoma: a review with emphasis on its fusion-driven biology. *Curr Oncol Rep*. 2018;20(5):37.
13. Nyquist KB, Panagopoulos I, Thorsen J, et al. Whole-transcriptome sequencing identifies novel IRF2BP2-CDX1 fusion gene brought about by translocation t(1;5)(q42;q32) in mesenchymal chondrosarcoma. *PLoS One*. 2012;7(11):e49705.
14. Dickson BC, Sung YS, Rosenblum MK, et al. NUTM1 gene fusions characterize a subset of undifferentiated soft tissue and visceral tumors. *Am J Surg Pathol*. 2018;42(5):636-645.
15. Zhu G, Benayed R, Ho C, et al. Diagnosis of known sarcoma fusions and novel fusion partners by targeted RNA sequencing with identification of a recurrent ACTB-FOSB fusion in pseudomyogenic hemangioendothelioma. *Modern Pathol*. 2019;32(5):609-620.
16. Fanburg-Smith JC, Auerbach A, Marwaha JS, Wang Z, Rushing EJ. Reappraisal of mesenchymal chondrosarcoma: novel morphologic observations of the hyaline cartilage and endochondral ossification and beta-catenin, Sox9, and osteocalcin immunostaining of 22 cases. *Hum Pathol*. 2010;41(5):653-662.
17. Bishop MW, Somerville JM, Bahrami A, Kaste SC, Interiano RB, Wu J, Mao S, Boop FA, Williams RF, Pappo AS, Samant S Mesenchymal chondrosarcoma in children and young adults: a single institution retrospective review. *Sarcoma* 2015;2015:608279, 1, 6.
18. Abbas M, Ajrawi T, Tungekar MF. Mesenchymal chondrosarcoma of the thyroid -- a rare tumour at an unusual site. *APMIS*. 2004;112(6):384-389.
19. Cesari M, Bertoni F, Bacchini P, Mercuri M, Palmerini E, Ferrari S. Mesenchymal chondrosarcoma an analysis of patients treated at a single institution. *Tumori*. 2007;93(5):423-427.
20. Xu J, Li D, Xie L, Tang S, Guo W. Mesenchymal chondrosarcoma of bone and soft tissue: a systematic review of 107 patients in the past 20 years. *PLoS One*. 2015;10(4):e0122216.
21. Schneiderman BA, Kliethermes SA, Nystrom LM. Survival in mesenchymal chondrosarcoma varies based on age and tumor location: a survival analysis of the SEER database. *Clin Orthop Relat Res*. 2017;475(3):799-805.
22. Pellitteri PK, Ferlito A, Fagan JJ, Suárez C, Devaney KO, Rinaldo A. Mesenchymal chondrosarcoma of the head and neck. *Oral Oncol*. 2007;43(10):970-975.
23. Doyle LA, Vivero M, Fletcher CD, Mertens F, Hornick JL. Nuclear expression of STAT6 distinguishes solitary fibrous tumor from histologic mimics. *Modern Pathol*. 2014;27(3):390-395.
24. Demicco EG, Harms PW, Patel RM, et al. Extensive survey of STAT6 expression in a large series of mesenchymal tumors. *Am J Clin Pathol*. 2015;143(5):672-682.
25. Shibuya R, Matsuyama A, Nakamoto M, Shiba E, Kasai T, Hisaoka M. The combination of CD99 and NKX2.2, a transcriptional target of EWSR1-FLI1, is highly specific for the diagnosis of Ewing sarcoma. *Virch Archiv*. 2014;465(5):599-605.
26. Granter SR, Renshaw AA, Fletcher CD, Bhan AK, Rosenberg AE. CD99 reactivity in mesenchymal chondrosarcoma. *Hum Pathol*. 1996;27(12):1273-1276.
27. Machado I, Navarro S, Picci P, Llombart-Bosch A. The utility of SATB2 immunohistochemical expression in distinguishing between osteosarcomas and their malignant bone tumor mimickers, such as Ewing sarcomas and chondrosarcomas. *Pathol Res Pract*. 2016;212(9):811-816.
28. Sharma AE, Pytel P, Cipriani NA. SOX9 and SATB2 immunohistochemistry cannot reliably distinguish between osteosarcoma and chondrosarcoma on biopsy material. *Hum Pathol*. 2022;121:56-64.
29. Murshed KA, Ammar A. Hybrid sclerosing epithelioid fibrosarcoma/low grade fibromyxoid sarcoma arising in the small intestine with distinct HEY1-NCOA2 gene fusion. *Pathology*. 2020;52(5):607-610.

How to cite this article: Xu B, Rooper LM, Dermawan JK, et al. Mesenchymal chondrosarcoma of the head and neck with *HEY1::NCOA2* fusion: A clinicopathologic and molecular study of 13 cases with emphasis on diagnostic pitfalls. *Genes Chromosomes Cancer*. 2022;61(11):670-677. doi:10.1002/gcc.23075